Supporting Information

# A Self-Adapting Hydrogel to Improve the Therapeutic Effect in Wound-Healing

*Yongsan Li,*[a, b] *Xing Wang,*[a,*] *Ya-nan Fu,*[a] *Yen Wei,*[b] *Lingyun Zhao,*[c,*] *Lei Tao*[b,*]

[a] Beijing Laboratory of Biomedical Materials, Beijing University of Chemical Technology, Beijing 100029, PR China.

[b] The Key Laboratory of Bioorganic Phosphorus Chemistry & Chemical Biology (Ministry of Education), Department of Chemistry, Tsinghua University, Beijing 100084, PR China.

[c] Key Laboratory of Advanced Materials, Ministry of Education, Institute of Regenerative Medicine and Biomimetic Material Science and Technology, Tsinghua University, Beijing 100084, PR China.

* E–mail:

leitao@mail.tsinghua.edu.cn; wangxing@mail.buct.edu.cn; lyzhao@mail.tsinghua.edu.cn

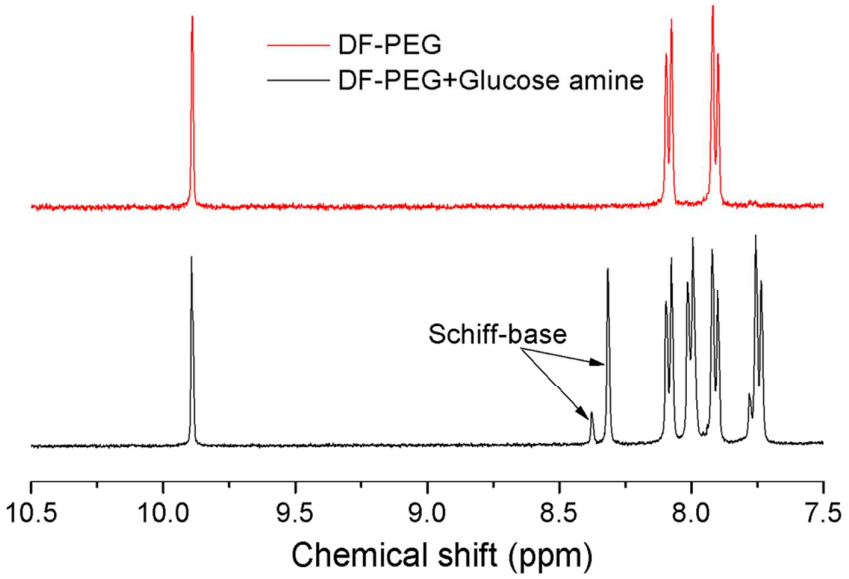


**Fig. S1 $^{1}$H NMR spectrum of Schiff-base.**

**Table S1.** The chart of chemical equilibrium constant calculated by the integration of DF-PEG.

| $m^{0}_{(DF\text{-}PEG)}$ | 1 | 2 | 4 |
|---|---|---|---|
| $S_{(DF\text{-}PEG)}$ | 385 | 477 | 1276 |
| $S_{(Schiff\text{-}base)}$ | 631 | 784 | 2096 |
| K | 70.65 | 70.85 | 70.80 |

$^{1}$H NMR was used to confirm the Schiff-base in CP hydrogel, glucosamine (GSA), the basic unit of chitosan, was employed as a model molecule to react with DF-PEG. As shown in Fig. S1, the significant peak of Schiff-base could be noticed. The integral ratio of Schiff-base and the unreacted benzaldehyde at DF-PEG chain ends was used to calculate the Keq (~ 70.8) of the reaction (Table S1).

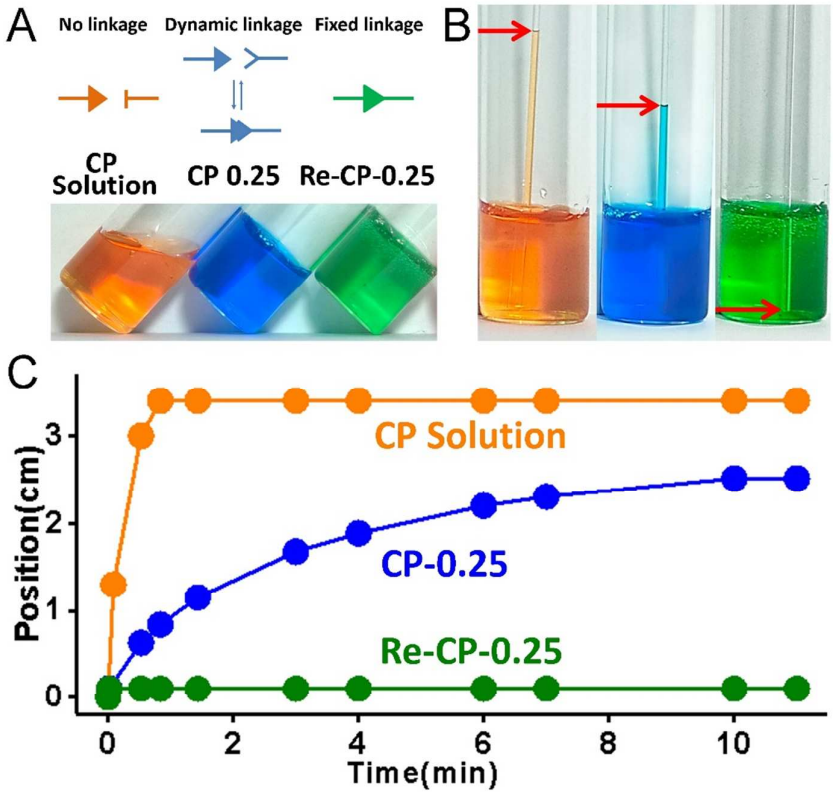


**Fig. S2** Capillarity experiments. (A) The inclined-tube test of the solution and hydrogels. (B) Capillary experiment of the CP solution (orange), CP-0.25 hydrogel (blue) and Re-CP-0.25 hydrogel (green). (C) Position vs time of Re-CP-0.25 hydrogel, CP-0.25 hydrogel and CP solution during the capillary experiments.

A capillary tube (diameter: 1.0 mm) was inserted into 2 mL of solid CP-0.25 hydrogel, the gel levels at different time points were recorded. Same procedure was repeated with Re-CP-0.25 hydrogel and a solution containing chitosan and dihydroxyl PEG (referred as the CP solution as the control). The thereof obtained position vs time plots were shown in Fig. S2C.

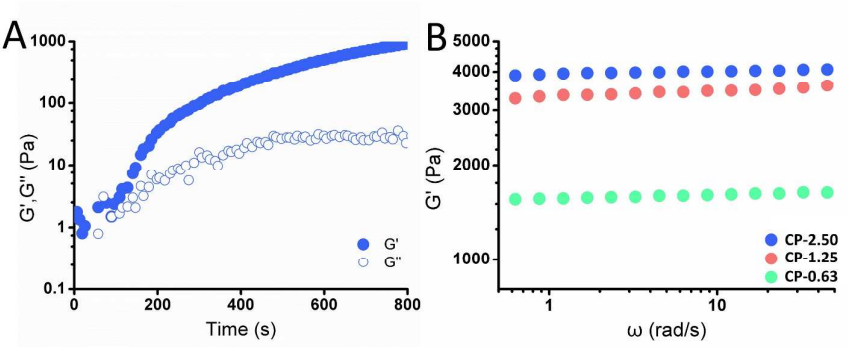


**Fig. S3** (A) Rheology analyses (0.1% strain and 6.3 rad $s^{-1}$) of the storage modulus G' (solid) and the loss modulus G'' (hollow) versus time during mixing the glycol chitosan (2.25wt%) and DF-PEG (2.50wt%). (B) Rheology analyses (0.1% strain and 6.3 rad $s^{-1}$) of the storage modulus G' versus frequency of the hydrogels with the same wt% glycol chitosan and different wt% DF-$PEG_{4000}$.

CPT hydrogels with different storage modulus could be obtained by just tuning the amount of DF-PEG (0.63% or 1.25%) in the hydrogels (Fig. S3).

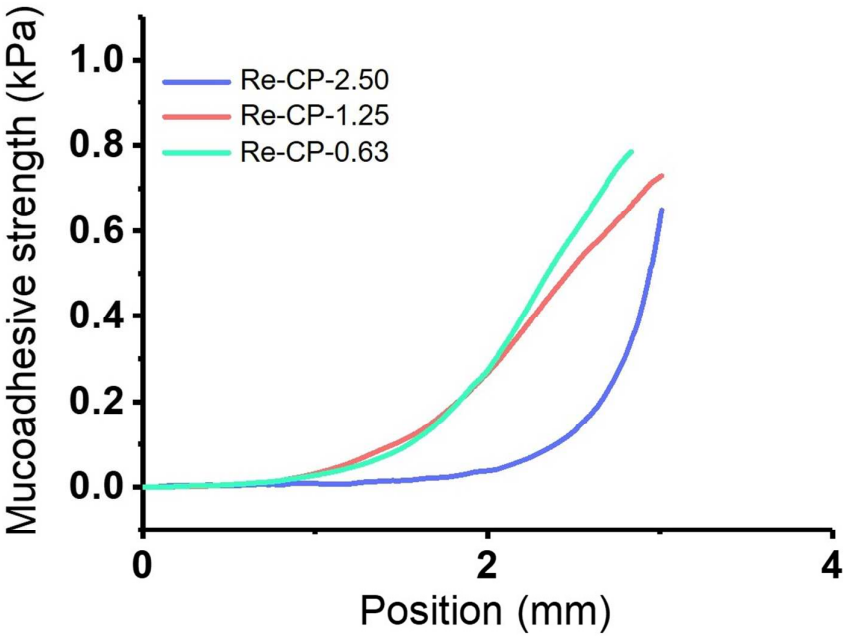

**Fig. S4** The mucoadhesiveness test of the Re-CP-0.25 hydrogel.

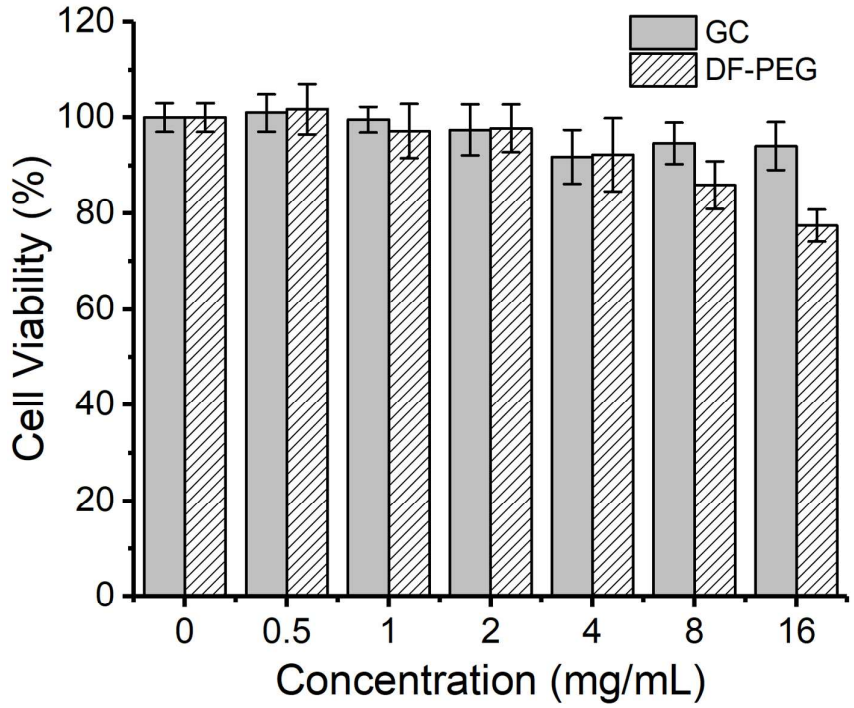


**Fig. S5** The cytotoxicity test of the glycol chitosan (GC) and DF-PEG.

The cytotoxicity tests of the glycol chitosan (GC) and DF-PEG were carried out on L929 cells using CCK-8 counting kit.

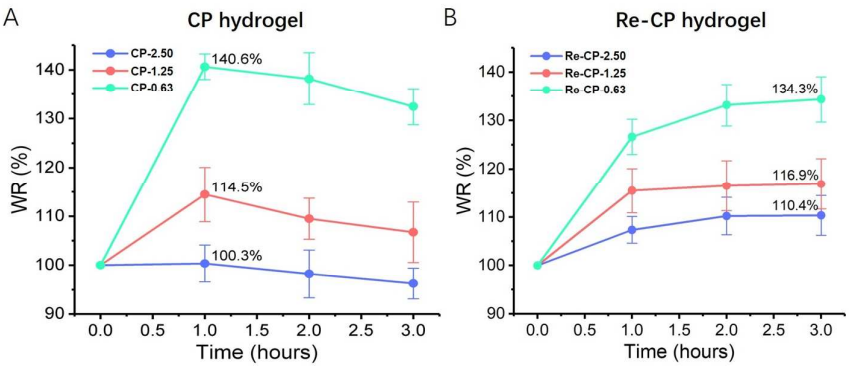


**Fig. S6** The swelling ratio of the hydrogels.

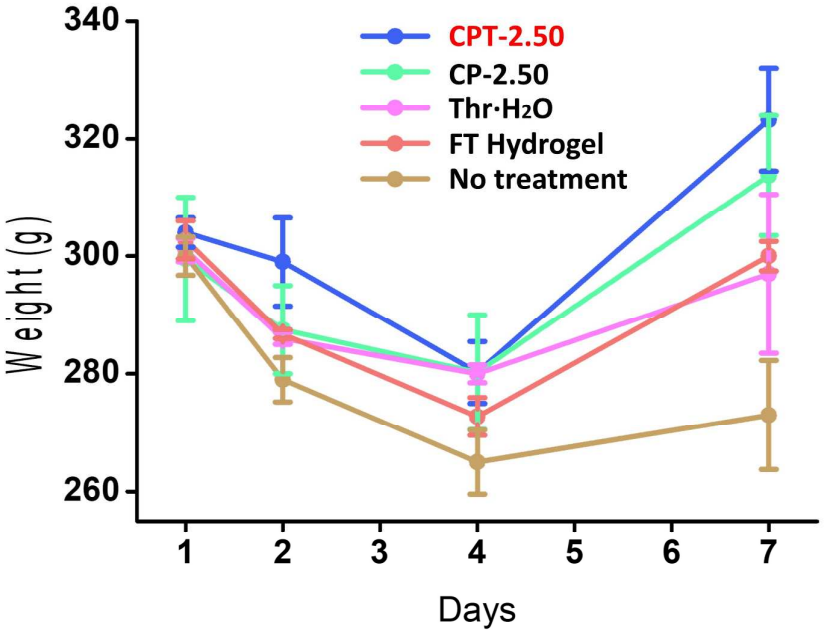


**Fig. S7** Rat weight changes during the experimental period. Data values correspond to means ± SD (n = 6).

The weights of rats after surgery were recorded on the 2nd 4th and 7th day (Fig. S7).

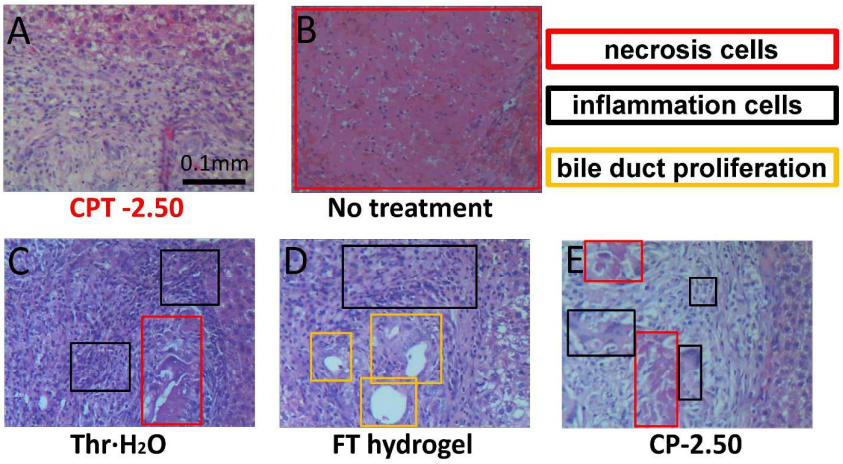


**Fig. S8** H&E histological examination of rats treated with (A) the CPT-2.50 hydrogel, (B) no treatment, (C) the thrombin solution, (D) the FT hydrogel, and (E) the CP-2.50 hydrogel at the 7th day after implantation. Cells shown in coloured boxes denote the following: red, necrosis

cells; black, inflammation cells including neutrophils and lymphocyte cells; orange, bile duct proliferation.

Histological sections of the regenerated liver tissue were stained by Hematoxylin and Eosin (H&E) to further evaluate the healing effect in each group. For the CPT-2.50 hydrogel treated group, the regenerated cells were well organized without hepatic necrosis (Fig. S8A). In the negative control group (Fig. S8B), large areas of hepatic necrosis were observed, and severe multinuclear giant cells almost covered the entire view, indicating high-level trauma was caused by the surgery. In the Thr·$H_2O$ group, severe inflammation and large areas of necrosis were observed (Fig. S8C). Inflammation and necrosis were also found in the FT hydrogel group, as was obvious bile duct proliferation (Fig. S8D). Partial inflammation with numerous neutrophils and macrophages, necrosis and bile duct proliferation were clearly visible in the CP-2.50 hydrogel treated group (Fig. S8E).